BLED WORKSHOPS
IN PHYSICS
VOL. 14, NO. 1
p. 57

Proceedings of the Mini-Workshop
Looking into Hadrons
Bled, Slovenia, July 7 - 14, 2013

Real and virtual Compton scattering experiments at MAMI and Jefferson Lab

S. Širca[a,b]

[a] Faculty of Mathematics and Physics, University of Ljubljana, Jadranska 19, 1000 Ljubljana, Slovenia
[b] Jožef Stefan Institute, Jamova 39, 1000 Ljubljana, Slovenia

Abstract. Real and virtual Compton scattering are among the most elementary electromagnetic processes on the proton. Two active directions of experimental pursuits are described: virtual Compton scattering experiment at Mainz aiming at the determination of proton generalized polarizabilities, and a recent initiative at Jefferson Lab to enrich the existing data set on real Compton scattering by extending it to higher s and t.

1 Virtual Compton scattering at low Q^2

Virtual Compton scattering (VCS) is a generalization of Compton scattering from real to virtual photons, i. e. the photon in the final state of the scattering process is electro-produced by inelastic scattering of electrons on protons:

$$e + p \longrightarrow e' + p + \gamma\,.$$

(The kinematics is indeed quite similar to pure elastic scattering. The final-state photon is identified by missing-mass technique.) The two nucleon static scalar polarizabilities measured by scattering of real photons, the electric α_E and the magnetic β_M, become *generalized polarizabilities*, $\alpha_E \to \alpha_E(Q^2)$, $\beta_M \to \beta_M(Q^2)$. The leading-order Feynman graphs corresponding to VCS are shown in Fig. 1.

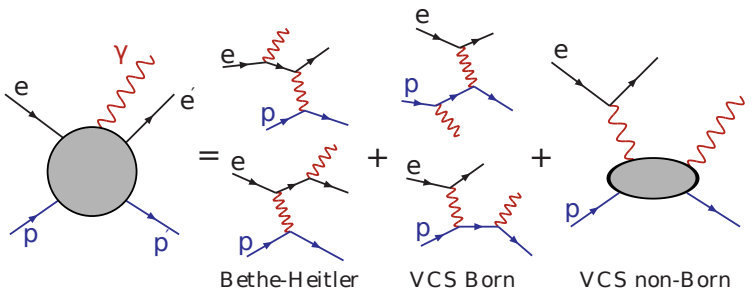

Fig. 1. Leading-order Feynman graphs for virtual Compton scattering.

1.1 Low-energy expansion

There are two main theoretical tools to analyze the VCS process. Both are aimed at the extractions of polarizabilities by comparing the calculated and measured cross-sections in an intricate fit procedure. In the approach that exploits the **low-energy theorem** (LET or "LEX") [1,2] one needs to stay below the pion production threshold. In LEX, the differential cross-section is expanded to first power of outgoing photon momentum in the center of mass:

$$d^5\sigma = d^5\sigma_{BH+B} + (\Phi q'_{cm}) \left[v_{LL} \left(P_{LL} - \frac{P_{TT}}{\varepsilon} \right) + v_{LT} P_{LT} \right] + \mathcal{O}\left(q'^2_{cm}\right) ,$$

where $d^5\sigma = d^5\sigma/dk'_{lab}d\Omega'_{lab}d\Omega_{\gamma cm}$ (there are also other options for combinations of independent variables). The main point is that $d^5\sigma_{BH+B}$ contains no polarizability effect and is "exactly" calculable if one assumes that the proton elastic form-factors are well known. Hence, by a simultaneous fit to the measured cross-section divided by the cross-section expanded to lowest order in q' over a large mesh of the photon emission angles one obtains the VCS response (or structure) functions $P_{LL} - P_{TT}/\varepsilon$ and P_{LT} that contain specific combinations of generalized and spin polarizabilities:

$$P_{LL} - \frac{P_{TT}}{\varepsilon} = \frac{4m_p}{\alpha} G_E^p\left(Q^2\right) \alpha_E\left(Q^2\right) + [\text{spin} - \text{flip GPs}] ,$$
$$P_{LT} = -\frac{-2m_p}{\alpha} \sqrt{\frac{q^2_{cm}}{Q^2}} G_E^p\left(Q^2\right) \beta_M\left(Q^2\right) + [\text{spin} - \text{flip GPs}] .$$

Note that additional assumptions on spin-flip polarizabilities are needed in order to extract α_E and β_M.

1.2 Dispersion-relations analysis

The second approach relies on **dispersion relations** ("DR") [3, 4] and is — in principle — applicable above the pion threshold if enough information on cross-sections for processes other than VCS are available. This method yields structure functions *as well as* polarizabilities $\alpha_E(Q^2)$ and $\beta_M(Q^2)$. The non-Born amplitudes are computed in terms of dispersive integrals, while the πN part (above the pion production threshold) is given by the $\gamma^\star N \to \pi N$ multipoles as obtained from the MAID unitary isobar model. The spin generalized polarizabilities are fixed, while the scalar ones have an unconstrained part which must be parameterized, typically in dipole forms like

$$\alpha_E(Q^2) - \alpha_E^{\pi N}(Q^2) = \frac{\alpha_E(0) - \alpha_E^{\pi N}(0)}{\left[1 + \frac{Q^2}{\Lambda_\alpha^2}\right]^2}$$

for the electric and similarly for the magnetic polarizability. Ultimately Λ_α^2 and Λ_β^2 are extracted from experimental data.

Only a few measurements of the VCS structure functions $P_{LL} - P_{TT}/\varepsilon$ and P_{LT} exist. Figure 2 shows the world supply of data. Apart from the real-photon values, there are the low-Q^2 measurements by the OOPS Collaboration from MIT-Bates [6], previous measurements at $Q^2 = 0.33\,(\mathrm{GeV}/c^2)$ by the A1 Collaboration at MAMI [7, 8], as well as the high-Q^2 data points from Jefferson Lab [9]. The programme to determine $P_{LL} - P_{TT}/\varepsilon$ and P_{LT} at various values of Q^2 in a single group of runs, and in turn to extract the generalized polarizabilities $\alpha_E(Q^2)$ and $\beta_M(Q^2)$, is presently underway at MAMI [5]. The aim is to provide additional and more precise data points at $Q^2 = 0.1$, 0.3 and $0.5\,(\mathrm{GeV}/c^2)$. The measurements will be performed in-plane, out-of-plane, and at low-q′ normalization settings in order to better control the systematics.

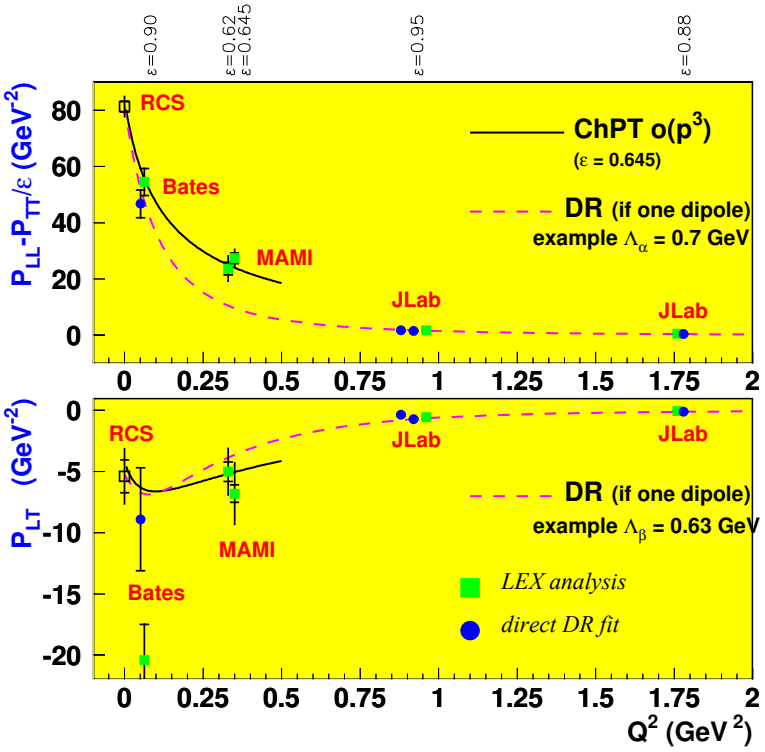

Fig. 2. The world supply of data for the structure functions $P_{LL} - P_{TT}/\varepsilon$ and P_{LT} for virtual Compton scattering on the proton. (Figure courtesy of H. Fonvieille.)

2 Real Compton scattering at high s and t

Compton scattering on the proton, in particular in its wide-angle regime where $s, -t, -u \gg M^2$, is a powerful and under-utilized probe of nucleon structure. As the process involves only real photons and only the ground state of the proton in

both initial and final states, it is elegantly simple. The physics involved is closely related to elastic electron-proton elastic scattering or DVCS, yielding the electromagnetic response of the nucleon without complications due to presence of other hadrons. However, wide-angle Compton scattering (WACS) remains one of the least understood fundamental processes in the several-GeV regime.

Several approaches to WACS have been proposed over the years, ranging from relativistic constituent quark models, investigations of the two-gluon exchange mechanism within pQCD, studies of the handbag mechanism in terms of generalized parton distributions (GPDs) [10] and, most recently, soft collinear effective theory [11]. In spite of the progress on all these fronts, WACS continues to pose many questions. Does large $-t$ ensure dominance of short-distance physics? What factorization scheme is valid? Is it true that the WACS reaction proceeds through the interaction of a photon with individual quarks? What information on the structure of proton can be extracted from the measurement of WACS form-factors? Given the fact that pQCD is not expected to be valid at this kinematic scale, why are the scaling predictions (see e.g. [12, 13]) so close to the observed values?

2.1 Factorization schemes in real Compton scattering

Obviously a thorough understanding of the possible underlying factorization schemes in real Compton scattering (RCS) is needed. In these schemes, the "hard scale" implies that all Mandelstam variables, s, $-t$, and $-u$, are large compared to m_p^2 or, equivalently, the transverse momentum transfer, $p_\perp$, is large. Only in this regime the transition amplitude is expected to become factorized as a convolution of a perturbative hard scattering amplitude, which involves the coupling of the external photon to the active quarks, with an overlap of initial and final soft (non-perturbative) wave-functions, which describes the coupling of the active quarks to the proton:

$$T_{if}(s,t) = \Psi_f \otimes K(s,t) \otimes \Psi_i \,,$$

where $K(s,t)$ is the perturbative hard scattering amplitude and the Ψ's are the soft wave functions.

Different factorization schemes for RCS are distinguished by the number of active constituents participating in the hard scattering subprocess. Two are most common. The handbag mechanism involves only one active constituent, while the pQCD mechanism involves three. In any given kinematic regime, both mechanisms may contribute. At "sufficiently high" energy, the pQCD mechanism is expected to dominate, but the anticipated point of onset of this regime is not known.

2.2 Results of the JLab 6-GeV RCS experiments

Two groups of RCS experiments have been performed at Jefferson Lab with 6 GeV. The E99–114 experiment (Hall A, 2002) yielded spin-averaged cross-sections over a broad kinematic range $6.8 < s < 11\,\mathrm{GeV}^2$, $2 < -t < 7\,\mathrm{GeV}^2$ [12], as well as polarization transfer asymmetries K_{LL} and K_{LT} at $s = 6.9\,\mathrm{GeV}^2$, $-t = 4\,\mathrm{GeV}^2$ [13].

The E07–002 experiment (Hall C, 2008) measured polarization observables K_{LL}, K_{TT} and P_N at $s = 8.0\,\mathrm{GeV}^2$, $-t = 2.1\,\mathrm{GeV}^2$ (analysis in progress). In spite of the immense increase in precision over older experiments from Cornell, and first measurements of RCS polarization observables ever, the factorization scheme issue could not be resolved unambiguously. There is evidence for factorization of the reaction mechanism and dominance of the handbag mechanism, but it is still inconclusive. As in elastic electron-proton scattering, the polarization observables in RCS have added insight: the process appears to strongly favor the leading-quark mechanism ($x \approx 1$), but some kinematic points have not satisfied the wide-angle condition ($s, -t, -u \gg M^2$) due to small value of $-u$.

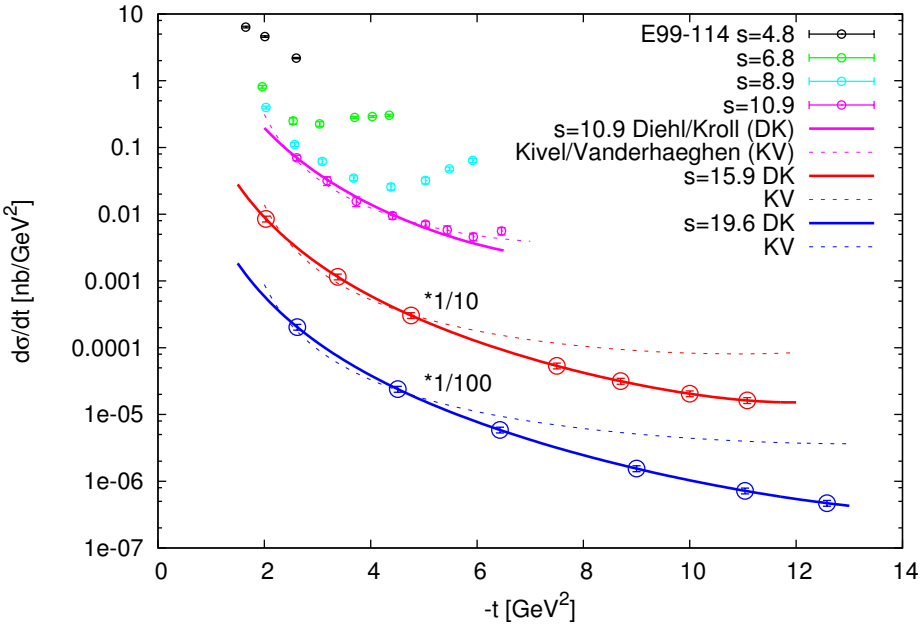

Fig. 3. The anticipated results in the proposed WACS experiment (the points at $s = 15.9$ and $19.6\,\mathrm{GeV}^2$ plotted on the Diehl-Kroll parameterizations of cross-sections). Only the statistical uncertainties are shown.

2.3 Proposal for a JLab 12-GeV WACS experiment

To address the issues and avoid the deficiencies enumerated above, a new proposal has been forwarded for a measurement of WACS in Hall C that will exploit the forthcoming 12 GeV beam of CEBAF [14]. We intend to measure 13 kinematic points, with the main goal of determine the scaling power n of the cross-section in terms of s at fixed θ_{cm}, and from this information infer the dominant reaction mechanism. The most important feature of the experiment is the fulfillment of the wide-angle condition, i.e. $s, -t, -u \gg M^2$ will be satisfied in *all* settings. A broad

range in $-t$ will be covered, allowing us to extract the RCS form-factor $\mathcal{R}(t)$ and find solid evidence for factorization. The results will also provide constraints on GPDs at high Bjorken x and constraints on 2γ effects, which are also relevant for the interpretation of electron-proton elastic scattering at high Q^2. The kinematics range covered will be

$$15.0 < s < 21.0\,\mathrm{GeV}^2 \qquad 2.0 < -t < 12.0\,\mathrm{GeV}^2 \qquad 3.0 < -u < 15.3\,\mathrm{GeV}^2\,.$$

The expected uncertainties, as given in the PR–12–13–009 proposal, are shown in Fig. 3. This proposal has been deferred by JLab PAC 40. We are presently working on its revision and will submit the new version to PAC 41 in early 2014.

References

1. P. Guichon et al., Nucl. Phys. A **591** (1995) 606.
2. M. Vanderhaeghen et al., Phys. Lett. B **402** (1997) 243.
3. B. Pasquini et al., Eur. Phys. J. A **11** (2001) 185.
4. D. Drechsel et al., Phys. Rep. **378** (2003) 99.
5. H. Fonvieille (spokesperson) et al. (A1 Collaboration), MAMI Proposal A1/1–09.
6. P. Bourgeois et al., Phys. Rev. Lett. **97** (2006) 212001.
7. J. Roche et al. Phys. Rev. Lett. **85** (2000) 708.
8. P. Janssens et al., Eur. Phys. J. A **37** (2008) 1.
9. G. Laveissière et al., Phys. Rev. Lett. **93** (2004) 122001.
10. M. Diehl, P. Kroll, `arXiv:1302.4604[hep-ph]`.
11. N. Kivel, M. Vanderhaeghen, `arXiv:1212.0683[hep-ph]`.
12. A. Danagoulian et al., Phys. Rev. Lett. **98** (2007) 152001.
13. D. J. Hamilton et al., Phys. Rev. Lett. **94** (2005) 242001.
14. B. Wojtsekhowski, D. Hamilton, S. Širca (spokespersons), Jefferson Lab Proposal PR–12–13–009 (submitted to PAC 40).